

SUPPLEMENTARY MATERIAL TO:
ROSEMARY FLETCHER, LAWRENCE BARHAM, GEOFF DULLER & MAYANK JAIN
NOTHING SET IN STONE: CHAÎNES OPÉRATOIRES OF LATER STONE AGE SEQUENCES FROM THE
LUANGWA VALLEY AND MUCHINGA ESCARPMENT, ZAMBIA

South African Archaeological Bulletin 77 (217): 89–114, 2022

SAMPLE PREPARATION AND DOSE RATE DETERMINATION

Three samples for OSL measurement were collected by hammering opaque black plastic tubes into the cleaned face of the excavated section and sealing the ends of the tubes with tape to prevent the sediment from moving during transit back to the laboratory. In the laboratory, material from the ends of the tubes which may have been exposed to daylight at the time of sampling was removed and used to determine the radiation dose rate for the samples. The sediment from the inner part of the tube was processed to obtain quartz grains for luminescence analysis. Preparation involved removal of any organics or carbonates with H_2O_2 and HCl, respectively. In both cases, reagents were refreshed until no further reaction was seen. After drying, samples were then sieved to isolate grains from 90 to 150 μm . Quartz was isolated using sodium polytungstate to separate grains with densities between 2.62 and 2.70 g cm^{-3} . This quartz-rich fraction was then etched in 40% hydrofluoric (HF) acid for one hour. This etching removes any remaining feldspars and removes the outer alpha-irradiated shell of the grains. Finally, samples were rinsed in HCl to remove and fluorides that may have been precipitated during the HF etch. The 90–150 μm diameter quartz grains were used for optically stimulated luminescence (OSL) measurements.

The rate at which samples were exposed to radiation during burial was calculated from the concentration of uranium (U), thorium (Th) and potassium (K) measured for each sample. Measurements of these radionuclides was undertaken on sediment from the ends of the sample tubes. This sediment was dried and then milled to a fine powder in a ball mill. The beta dose rate was measured using a GM-25-5 beta counter (Bøtter-Jensen & Mejdahl 1988). A second set of measurements were made using Thick Source Alpha counting (TSAC). These yielded the concentration of U and Th (Table 1). The potassium concentration in the sediments was calculated by the difference between the measured beta activity and the beta activity calculated from the U and Th concentrations.

The cosmic dose rate to the samples was calculated using the equations of Prescott and Hutton (1994) based upon the longitude, latitude and altitude of the site, and the burial depth within the section. An additional consideration at this site is that the granite boulder that forms the rock shelter acts as additional shielding from cosmic rays. The final cosmic dose

rates used to determine ages (Table 1) were calculated by assuming that 80% of the sky view of the site was shielded by the 10 m thick granite boulder in addition to the sediment accumulated at the section, and the remaining 20% of the sky view was unaffected by the granite boulder. At this site, the high concentration of radionuclides means that the cosmic dose rate only makes up ~1.5% of the total dose rate.

The total dose rate to the quartz grains was the sum of the beta dose rate derived from beta counting, the gamma dose rate derived from the concentrations of U, Th and K, and the cosmic dose rate (Table 1).

MEASUREMENTS DETAILS

Luminescence measurements to determine the equivalent dose for each sample were made on a Risø TL/OSL reader equipped with a single grain system (Bøtter-Jensen *et al.* 2003). Quartz grains were mounted in ten single grain discs for each of the three samples, giving a total of 1000 grains measured for each sample. An additional set of measurements were made on another ten single grain discs with sample SL33 for dose recovery. A green laser (532 nm) was used for all the single grain measurements in the Risø TL-OSL reader. OSL measurement lasted one second per grain, and the data were collected over 50 channels.

A Single Aliquot Regenerative dose (SAR) protocol was used with a preheat of 220°C for 10 s and a cutheat of 160°C. The regeneration doses varied between 4.8 to 95 Gy and a test dose of 2.4 Gy was used for sensitivity correction. Recycling was measured at 24 and 48 Gy; the latter was also measured with and without IR bleaching after the preheat and before OSL to detect possible feldspar grains using the OSL IR depletion ratio (Duller 2003).

To assess the SAR protocol, ten single grain discs of sample SL33 were used to undertake a dose recovery experiment to see whether a known laboratory radiation dose could be accurately measured. The experiment consisted of bleaching the signal from the grains, and then giving a known beta dose of 11.93 Gy. The samples were then measured using the SAR protocol described above.

ANALYSIS

For each OSL curve, the first five channels were used for the signal with the average of the last 25 channels subtracted as

TABLE 1. Dosimetry information for the three OSL samples. A grain size of 90–150 μm was used for all samples.

Sample (Aber90/)	Depth (cm)	Water content (%)	Alpha count rate (cts/ks/cm ²)	Beta dose (Gy/ka)	Calculated concentrations			Total dose (Gy/ka)
					K (%)	U (ppm)	Th (ppm)	
SL31	31	5 ± 2	1.52 ± 0.02	3.70 ± 0.12	2.74 ± 0.23	5.99 ± 0.79	22.98 ± 2.65	5.56 ± 0.21
SL32	62	8 ± 2	1.70 ± 0.02	3.75 ± 0.12	2.57 ± 0.20	6.95 ± 0.62	24.71 ± 2.08	5.56 ± 0.18
SL33	109	10 ± 5	1.39 ± 0.02	2.97 ± 0.10	1.94 ± 0.16	6.37 ± 0.52	17.71 ± 1.74	4.31 ± 0.21
Sample (Aber90/)	Number of grains		Central Age Model		Maximum Dose Model			
	Measured	Accepted	D_e (Gy)	Age (ka)	D_e (Gy)	Age (ka)		
SL31	1000	406	8.86 ± 0.28	1.60 ± 0.08	22.6 ± 0.98	4.06 ± 0.23		
SL32	1000	331	12.3 ± 0.27	2.21 ± 0.09	20.9 ± 0.79	3.76 ± 0.19		
SL33	1000	209	16.7 ± 0.52	3.88 ± 0.22	29.6 ± 1.41	6.88 ± 0.47		

the background. Most grains showed an OSL signal dominated by the fast component (Jain *et al.* 2003). Dose response curves were fitted with a single saturating exponential curve (Equation 1) in Analyst (Duller 2015) to obtain individual estimates of equivalent dose (D_e).

$$I = a \left(1 - e^{-\left(\frac{D}{D_0}\right)} \right) \quad (1)$$

where I is the luminescence signal, D is the regeneration dose, and a and D_0 are fitted parameters. Data from single grains were screened using three criteria, and only accepted if (a) D_e was less than or equal to two times D_0 (characteristic dose), (b) if the recycling ratio (including its 1σ uncertainty) was within 10% of unity, and (c) if the IR OSL depletion ratio (including its 1σ uncertainty) was within 10% of unity. After application of these criteria between 209 and 406 D_e values were obtained.

RESULTS

The dose recovery experiment on sample SL33 produced a recovery ratio of 0.99 ± 0.01 (mean $\pm 1\sigma$ standard error), demonstrating that the SAR protocol applied to this quartz can accurately measure a radiation dose (Fig. 1(a)). The overdispersion of this dose recovery data was 5%. The dose distributions for the three samples are shown in Fig. 1(b) on an abanico plot (Dietze *et al.* 2016). The distributions are rather broad with overdispersion values ranging from 37–62% (Table 1), but the probability density plot of the D_e values for each of the three samples shows a clear peak (shown on the right-hand side of Fig. 1(b)), and the position of this peak increases to higher doses with depth in the section as would be expected. Some, or all, of the overdispersion seen in the samples may be due to variations in dose rate to individual grains (*cf.* Burrough *et al.* 2019), but there is also evidence of bioturbation at the site today (e.g. ant burrows) which may have moved sediment grains vertically through the section.

Two age models have been applied to the dose distributions and the results of these are shown in Fig. 1(b) and (c) and listed in Table 1. The first is the Central Age Model (CAM, Galbraith *et al.* 1999) which is a measure of central tendency and would be appropriate if it is assumed that the scatter is primarily due to variations in dose rate (Fig. 1(b)). The second model is the Maximum Dose Model (MDM, Olley *et al.* 2006) which would be appropriate if bioturbation is the dominant process leading scatter and the primary impact of this bioturbation has been to introduce grains from the surface which have been bleached and therefore underestimate the depositional age of the sediment (Fig. 1(c)). The ages for SL31 and SL32 using the MDM are in reverse chronostratigraphic order, though they overlap within uncertainties. In contrast the ages for all three samples obtained using CAM (Table 1) are stratigraphically consistent and describe an accumulation rate of 0.24 m/ka at the site. It is difficult to rule out bioturbation having an impact on the OSL data, and the MDM ages provide an upper limit for the ages. However, given the stratigraphic consistency of the CAM ages and the unimodal distributions (Fig. 1(b)), the CAM ages appear to be the most accurate for these sediments.

REFERENCES

- Bøtter-Jensen, L., Andersen, C.E., Duller, G.A.T & Murray, A.S. 2003. Developments in radiation, stimulation and observation facilities in luminescence measurements. *Radiation Measurements* 37(4–5): 535–541.
 Bøtter-Jensen, L. & Mejdaal, V. 1988. Assessment of beta dose-rate using a GM multicontainer system. *Nuclear Tracks and Radiation Measurements* 14: 187–191.

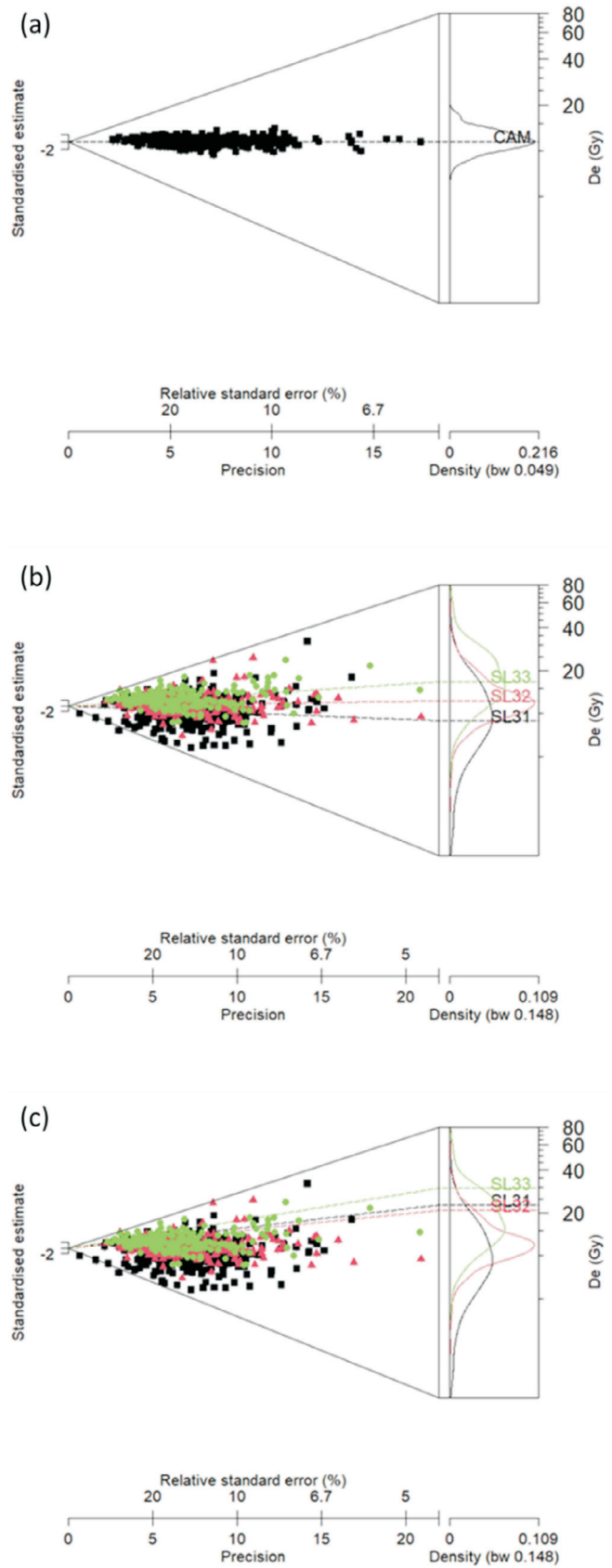


FIG. 1. Abanico plots showing individual D_e data for: (a) the dose recovery experiment on SL33 with a given dose of 11.93 Gy ; (b) All three samples from Poacher's Cave (shown in different colours) with the Central Age Model (CAM) value shown as a dashed line and labelled with the name of each sample; and (c) the same data as shown in (b) but with the Maximum Dose Model values shown by the dashed lines.

- Burrough, S.L., Thomas, D.S.G. & Barham, L. 2019. Implications of a new chronology for the interpretation of the Middle and Later Stone Age of the upper Zambezi Valley. *Journal of Archaeological Science: Reports* 23: 376–389.
- Dietze, M., Kreutzer, S., Burow, C., Fuchs, M.C., Fischer, M. & Schmidt, C. 2016. The abanico plot: visualising chronometric data with individual standard errors. *Quaternary Geochronology* 31: 12–18.
- Duller, G.A.T. 2003. Distinguishing quartz and feldspar in single grain luminescence measurements. *Radiation Measurements* 37: 161–165.
- Duller, G.A.T. 2015. The Analyst software package for luminescence data: overview and recent improvements. *Ancient TL* 33(1): 35–42.
- Galbraith, R.F., Roberts, R.G., Laslett, G.M., Yoshida, H. & Olley, J.M. 1999. Optical dating of single and multiple grains of quartz from Jinmium rock shelter, northern Australia: Part I, Experimental design and statistical models. *Archaeometry* 41: 339–364.
- Jain, M., Murray, A.S. & Bøtter-Jensen, L. 2003. Characterisation of blue-light stimulated luminescence components in different quartz samples: implications for dose measurement. *Radiation Measurements* 37(4–5): 441–449.
- Olley, J.M., Roberts, R.G., Yoshida, H. & Bowler, J.M. 2006. Single-grain optical dating of grave-infill associated with human burials at Lake Mungo, Australia. *Quaternary Science Reviews* 25: 2469–2474.
- Prescott, J.R. & Hutton, J.T. 1994. Cosmic ray contributions to dose rates for luminescence and ESR dating: large depths and long-term time variations. *Radiation Measurements* 23: 497–500.